

Optical characterization of integrated P+/N-Well/P-substrate and N-Well/P-substrate photo-device structures on CMOS technology

G. Castillo-Cabrera¹, J. García-Lamont², M. A. Reyes-Barranca³, J. A. Moreno-Cadenas³ and A. Escobosa-Echavarría³

¹ESCOM-IPN, CINVESTAV-IPN, Mexico D.F., Mexico

²CITIS, Instituto de Ciencias Básicas e Ingeniería, Universidad Autónoma del Estado de Hidalgo., Méx.

³Department of Electrical Engineering, CINVESTAV-IPN, México D.F., México

Phone +52 (55) 5747-3776, E-mail: ¹gccbiology@hotmail.com

Abstract — Here, a characterization methodology for integrated silicon-based photo-devices is presented. Devices are phototransistors (“P+/N-Well/P-substrate”) and photodiodes (“N-Well/P-substrate”) with similar sizes, (9μmx9μm). They were integrated in a 1.5μm CMOS technology through MOSIS. Through these characterizations it is possible also to find out in general, the performance advantages and disadvantages, comparing measurements made on these kinds of structures. It was found that phototransistors have a better performance compared with photodiodes. The contribution from substrate leakage current in N-Well/P-substrate structures is high, as well as from carriers generated in the neighborhood of the pixel circuit. It is shown that crosstalk is the phenomenon that deviates the measured photo-response from the ideal model of photo-devices.

Keywords: Crosstalk, Phototransistor, Photodiode, Photosensitivity, Quantum efficiency

I. INTRODUCTION

CMOS technology for integrated circuits is a very well known process dedicated for electronic circuit fabrication and development. Nevertheless, photo-devices such as phototransistors and photodiodes can be fabricated too with this technology, making possible to implement systems for different applications on image sensing and processing. Despite the remarkable technology advances, as shrinkage of devices goes on there is still a lot of work to do to improve the performance regarding integrated photo-sensors, since the operation is still limited by issues like signal to noise ratio, dynamic range, fixed pattern noise and crosstalk. Furthermore, clinical and scientific applications are taking advantage on the development of prototype systems, like retinal prosthesis, for instance [1-3]. Although a great number of systems have been mainly developed based on CCD and BiCMOS technologies, there is the challenge to improve CMOS devices beyond actual limits. Thus, devices should be first evaluated toward image sensing applications, from where design parameters can be pointed out in order to maximize the performance of these photo-devices. Thereby, two feasible structures were studied: P+/N-Well/P-substrate (phototransistors) and N-Well/P-substrate (photodiodes).

Structures were fabricated through MOSIS with the 1.5μm AMI’s CMOS technology. Also, a simple architecture was used to implement a pixel that helps in the measurements of the chip through an integrated output buffer. So, a methodology is proposed that can be easily used and extrapolated to smaller CMOS technologies. Important features such as spectral response, photosensitivity and quantum efficiency can be measured for each integrated photo-device. Having in mind artificial retina prosthesis, the architecture should have few transistors, low power consumption and little integrated area. Besides, image processing using pulsed parallel image processing is highly recommended, so a block can be added at the output of this architecture, such as a pulsed frequency modulated (PFM) stage, to evaluate a prototype system.

II. METHODOLOGY

The chip contains five pairs of phototransistors and five pairs of photodiodes, with one instance of each pair covered with metal for dark current characterization purposes. Cells with the following areas were integrated: 100μmx100μm, 64μmx64μm, 32μmx32μm, 16μmx16μm and 9μmx9μm, but results here reported are only from those devices having an area of 9μmx9μm. Fig. 1 shows the cross section for both devices where the respective junctions are shaded and each terminal for the phototransistor and the photodiode is clearly indicated. Fig. 2 shows the layout proposed in this study for the measured devices.

The ring above the base area of the phototransistor has the same dimensions of the photodiode’s anode ring (9μmx9μm). The photocurrent generated is collected by the phototransistor’s emitter and the same happens with the cathode of the photodiode. Fig. 3 shows the schematic of the circuit used to convert the photocurrent to voltage so it can be later processed with PFM. The photo-device can be either a phototransistor or a photodiode. P-channel MOS transistors labeled as MREST and MSHUT operate as switches with driving signals configured for voltage integration at the gate of M1, while M2 selects the row in a pixel matrix array.

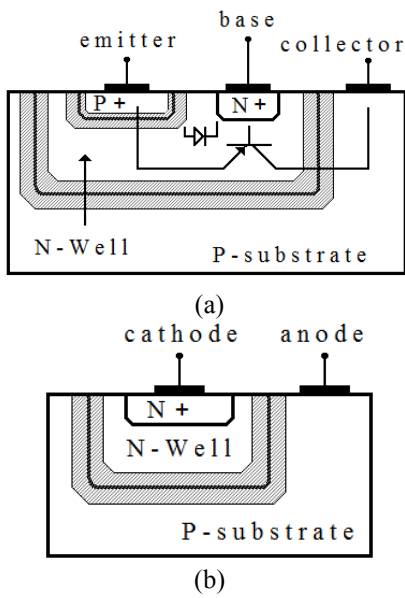


Fig. 1. Cross section of the analyzed structures. (a) P+/N-Well/P-substrate structure. (b) N-Well/P-substrate structure.

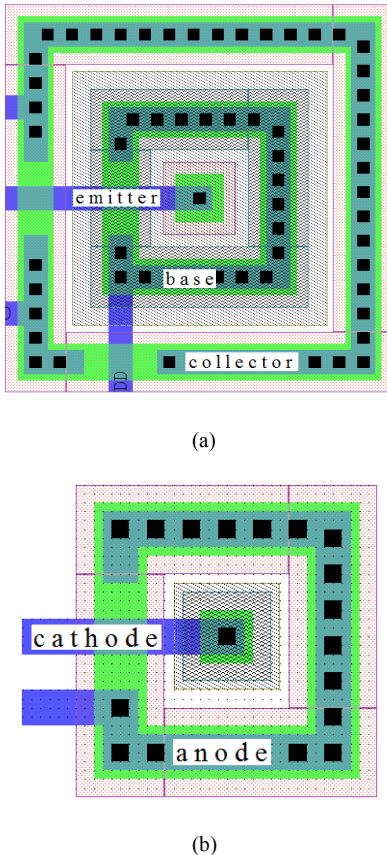


Fig. 2. Layout of (a) P+/N-Well/P-substrate structure (Phototransistor), (b) N-Well/P-substrate structure (Photodiode).

The DC voltage source, V_{reset} , is the reference voltage from which integration of the photocurrent takes place, with a voltage range of 2.15V – 3.5V. The current source I_{sc} is the load of the amplifier configured with M1 and M2 and voltage read out is taken at node 4. This amplifier has a very important feature that helps in the characterization of photo-devices, since it has a variable voltage gain. This allows establishing a DC operating point on the circuit, depending on the kind or size of the device under test. Fig. 4 shows the driving signals applied to the gate of MREST and MSHUT. M1, MREST and MSHUT has minimum aspect ratios based on the 1.5 μ m AMI's CMOS technology and M2 was designed with $W=64.8\ \mu m$ and $L=2.4\ \mu m$ so the voltage gain can be adjusted within a range of 10dB – 35dB, as shown in Fig. 5(a). Here, a simulation of the transfer function of the amplifier shows the different gains that can be achieved adjusting the current source, I_{sc} , giving an extra degree of freedom to the measurement of photo-devices of different size and operating with different biasing. Also, Fig. 5(b) shows the simulation of voltage integration at node 2, taken from node 4, where V_{out} is measured.

An important parameter to be measured regarding phototransistors or photodiodes is the photocurrent. So, from Fig. 3, and if the area of the illuminated reversed biased junction is known (see Figs. 1 and 2), the current density can be computed with the following expression:

$$J_{ph} = \frac{\Delta V \cdot C_{ph}}{\Delta t \cdot A_{ph}} \quad (1)$$

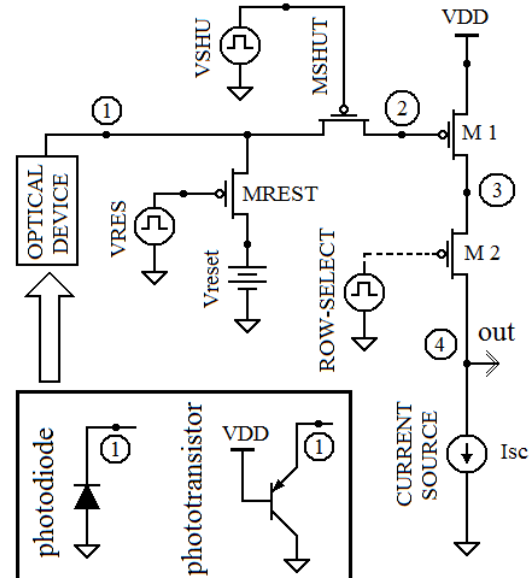


Fig. 3. Schematic circuit of the pixel used for photo-devices characterization.

where $\Delta V/\Delta t$ is the slope of the integrated voltage during Δt at node 2 (Δt is specified in Fig. 4). C_{ph} is the capacitance at the same node and A_{ph} is the area of the junction generating the photocurrent and both can be determined from the layout in Figure 2.

On the other hand, V_{out} is the voltage measured at node 4 in Fig. 3 and provided the voltage gain, Av , is known, then ΔV can be calculated with the following expression:

$$\Delta V = \frac{V_{out}}{Av} \quad (2)$$

About the device under test, either the anode of the photodiode or the collector of the phototransistor are connected to ground while the base is connected to $VDD=5V$, respectively. From the layout, the extracted capacitance, C_{ph} , is approximately 13.96 pF with a surface A_{ph} of $2.0 \times 10^{-10} \text{ m}^2$. Hence, photocurrent density can be estimated measuring the voltage at node 4 at the end of the integration time (see Fig 5(b)). This can be done at different light wavelengths from where the spectral response of photo-devices can be plotted.

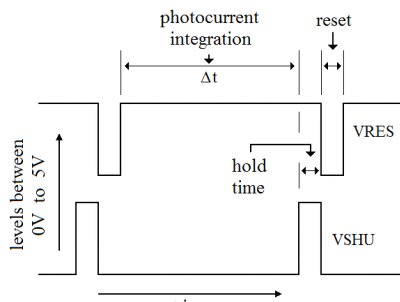


Fig. 4. Input signals at the gate of MREST and MSHUT.

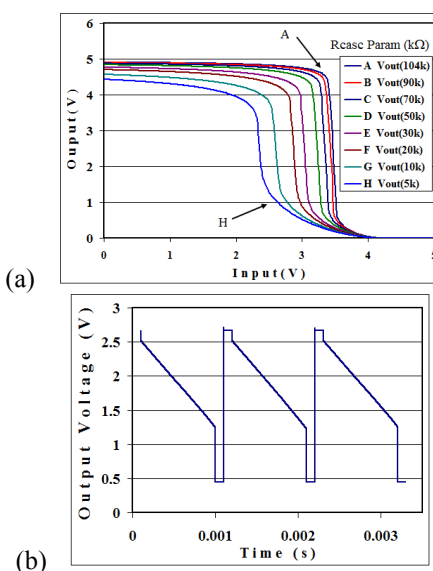


Fig. 5. (a) Transfer function of the pixel amplifier; (b) photocurrent integrated voltage.

A monochromator HILGER & WATTS and an ISA lamp were used in a set-up to measure V_{out} vs wavelength only in integrated phototransistors and photodiodes with area $9\mu\text{m} \times 9\mu\text{m}$. Equation (1) is used to calculate the corresponding current density.

III. RESULTS

Measurements

Five chips with phototransistors and photodiodes were measured and their corresponding photo-current-vs-wavelength plots are shown in Figs. 6 and Fig. 7.

Here it can be noticed the strong difference between the response of both devices. The spectral photo-response of photodiodes is almost one order of magnitude greater than the photo-response of phototransistors. This difference has been attributed to the phenomenon known as “crosstalk” [4]. Two physical mechanisms can cause crosstalk. First, the *optical crosstalk* is due to the phenomenon of reflection, refraction and scattering of light traveling through the SiO_2 and other layers like metals and silicon nitride. And second, the *electrical crosstalk*, the main contributor, is due to diffusion of minority carriers with long lifetime from neighboring devices [5-6]. So, it is demonstrated that with this technology used, the P+/N-Well/P-substrate structure is not so affected by crosstalk as the N-Well/P-substrate structure. Therefore, it can be assumed that phototransistors have a minor effect due to electrical crosstalk and the response is restricted just to what happens within the N-well region. The small oscillations on curves are believed to be caused due to Fabry-Perot interference among the different layers present on the devices [7, 8].

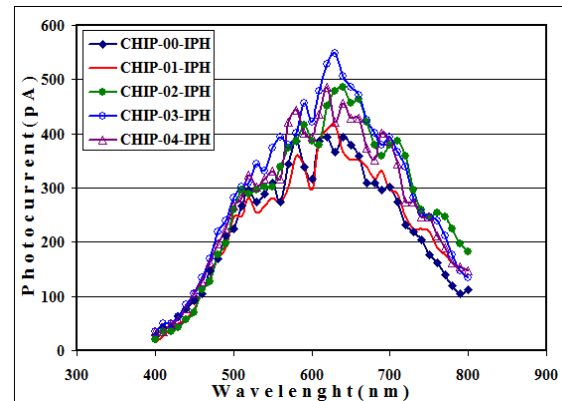


Fig. 6. Spectral photo-response of phototransistors.

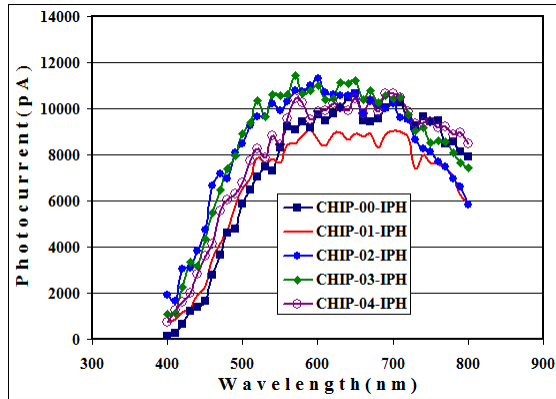


Fig. 7. Spectral photo-response of photodiodes.

Fig. 8 shows the power spectrum, P_{opt} , of the ISA lamp which was used to obtain the photosensitivity illustrated in Fig. 9 for phototransistors. The experimental photocurrent density was evaluated with Eq. (1). Photosensitivity and quantum efficiency (Figs. 9 and 10), were obtained with the following equations:

$$S_\lambda = \frac{J_{ph}}{P_{opt}} \quad (3)$$

where P_{opt} : optical power density from Fig. 8.

$$QE = S_\lambda \frac{h \cdot c}{\lambda \cdot q} = 1240 \frac{S_\lambda}{\lambda} \quad (4)$$

where hc/λ : energy of photons, with λ in μm .
 q : charge of electrons (Coul.).

IV. DISCUSSION

A). Lateral Crosstalk Mechanism

We have focused in the characterization and analysis of likely mechanisms that could contributes to the crosstalk on structures “P+/N-Well/P-substrate” (phototransistors) and “N-Well/P-substrate” (photodiodes). On these kinds of photo-devices, crosstalk has been defined and classified in two main mechanisms: (a) optical crosstalk and (b) electrical crosstalk [4-6]. Here, we introduce an additional classification of crosstalk, as is shown in the Fig. 11. The first classification is the lateral crosstalk mechanism which includes optical crosstalk (OC), and Lateral Electrical Crosstalk (LEC).

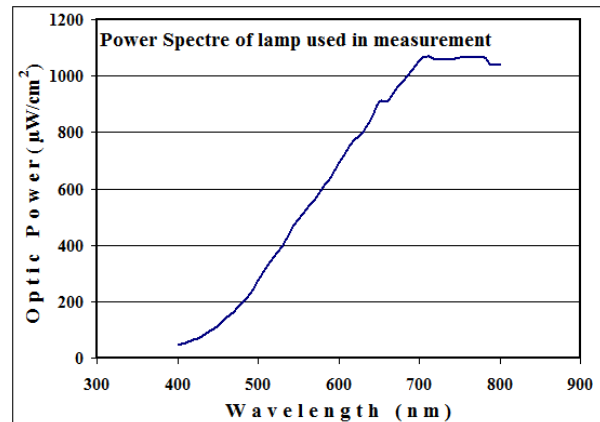


Fig. 8. Power spectrum of the ISA lamp.

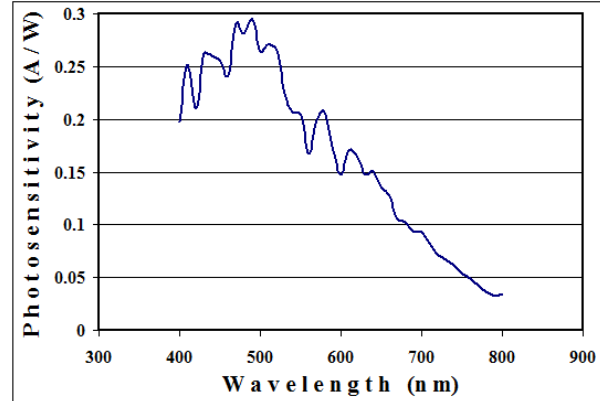


Fig. 9 Photosensitivity of phototransistor

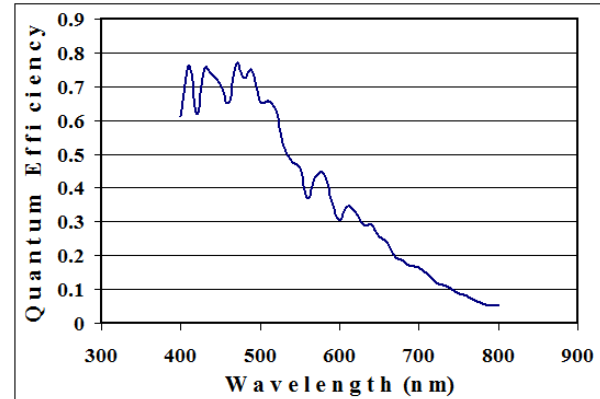


Fig. 10. Quantum efficiency in phototransistors

Optical crosstalk is due to light traveling laterally among the layers up to the junction (near the surface of the device) acting as a waveguide, as is shown in the Fig. 11. Lateral electrical crosstalk (LEC) is the phenomenon whereby photons generate carriers in the “**near to the surface region**”. That phenomenon has its origin in short wavelength light, mainly under of 650nm. Both, optical and LEC crosstalk, are present either in, phototransistors or photodiodes. However, in phototransistors this contribution is as photocurrent collected by the base contact, which is tied to VDD, masking the effect. This is a first reason whereby the photo-current is larger in photodiodes than in phototransistors. Fig. 11 shows the way in which both, OP and LEC mechanisms, affect the response of phototransistors.

In Fig. 12, we can see how both, OP and LEC, affect the response in the photodiode. The effect is very strong since the current comes from all directions.

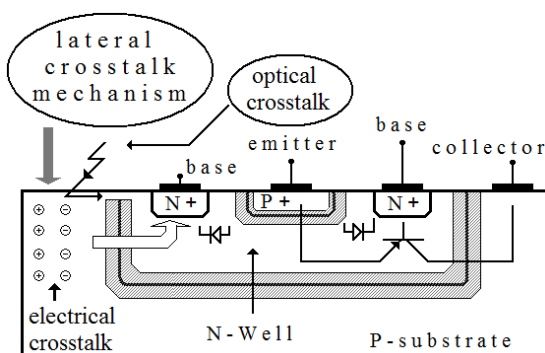


Fig. 11.- Lateral crosstalk mechanism in the phototransistor

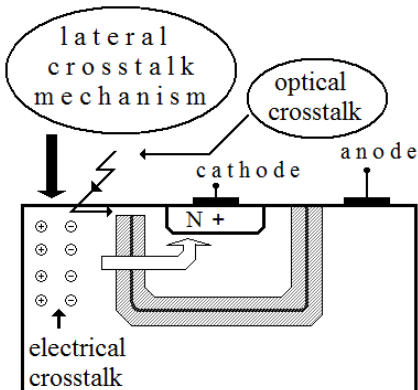


Fig. 12. Lateral crosstalk mechanism in the photodiode.

B). Vertical Crosstalk Mechanism

Vertical crosstalk mechanism is shown in Fig. 13. It originates only due to electrical crosstalk, so it is called vertical electrical crosstalk (VEC). In the case of phototransistors, carriers generated along the substrate, as well as behind and outside the “N-Well”, and are collected by the base contact since it is connected to a higher voltage than the emitter. So, only majority carriers are collected by the base.

In this case, diffusion of minority carriers is present as leakage current. Hence, little or no contribution to the spectral response of phototransistors is due to vertical electrical crosstalk. Vertical electrical crosstalk effect for the photodiode case is shown in the Fig. 14.

Carriers generated by photons behind and outside the N-Well contribute to the spectral response of the photodiode with the leakage current coming from the substrate.

Carriers generated deep in the substrate are due to longer wavelengths. This component of leakage current has a very strong effect over the photodiodes but this is not the case for phototransistors, so the difference appreciated in Figs. 6 and 7 can be attributed to this.

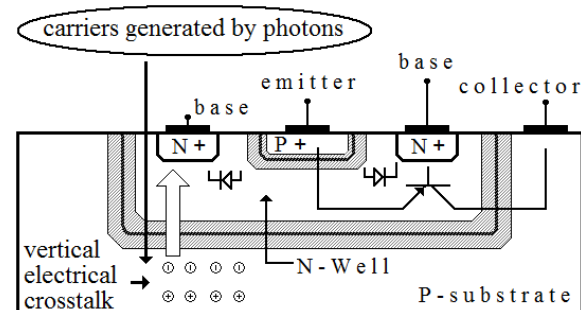


Fig. 13. Vertical Electrical Crosstalk mechanism in phototransistors

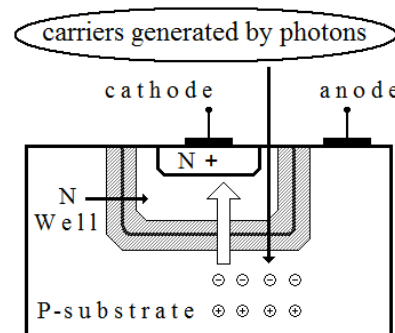


Fig. 14. Vertical Electrical Crosstalk mechanism in photodiodes

V. CONCLUSIONS

The proposed characterization methodology appears to be a convenient way for obtaining performance features of integrated photo-devices. Important parameters can be measured, as photocurrent generated, photosensitivity and quantum efficiency. Also, it can be identified operating limits regarding the geometric design of the photo-devices array that should be taken into consideration regarding the application given. More work should be done directed to identify problems related with optical cross-talk, as this seems to be an issue that depends on the layers used in the CMOS technology of fabrication. Our measurements show not only previous definitions about of phenomena of optical and electrical crosstalk, but also evidence of a very strong contribution from substrate's leakage currents in the case of photodiodes. In the case of phototransistors, we can say that the bias conditions are a key factor to minimize this contribution. For instance, if the base is tied to VDD, this helps to cancel out as much as possible the crosstalk contribution to photocurrent. Hence, the designer has to take into account whether this contribution should be minimized depending on the desired application, since an array with neighboring photo-devices may mask this phenomenon. This is because in many cases, it would be desirable that the response of optical devices has its origin only in well defined region. So we believe that this is the case for phototransistors here presented.

Even quantum efficiency and photosensitivity for phototransistors are not so high, this can be evidence that crosstalk is a minor contribution to the corresponding spectral response and it can be attributed only to photocurrent generated nearby the N-Well.

Photosensitivity and quantum efficiency plots for photodiodes were hard to estimate due to the strong effects of crosstalk since the converted voltage saturates the amplifier provided that integrated voltage could rise beyond VDD values. It should be remembered that low supply voltages is a trend in VLSI integrated circuits.

REFERENCES

- [1] M. S. Humayun, "Intraocular Retinal Prosthesis", *Tr. Am. Ophth. Soc.*, Vol. 99, pp. 271-300, 2001.
- [2] E. M. Maynard, "Visual Prostheses", *Annu. Rev. Biomed. Eng.*, Vol. 3, pp. 145-168, 2001.
- [3] X. Chai, L. Li, K. Wu, C. Zhou, P. Cao, and Q. Ren, "C-Sight Visual Prostheses for the blind, Optic Nerve Stimulation with Penetrating Electrode Array", *Biomedical Engineering in China, IEEE Engineering in Medicine and Biology Magazine, IEEE*, Vol. 27, Issue 5, pp. 20-28, 2008.
- [4] I. M. Kang, "The simulation of the crosstalk between Photodiodes Fabricated Using the $0.18\mu\text{m}$ CMOS Process", School of Electrical Engineering, Seoul National University, in SMDL Annual Report 2002.
- [5] M. Tabet, "Double Sampling Techniques for CMOS Image Sensors", Doctor of Philosophy thesis, University of Waterloo Electrical and Computer Engineering. Waterloo, Ontario, Canada, 2002.
- [6] I. Brouk, Y. Nemirovsky, S. Lachowicz, E. A. Gluszak, S. Hinckley, and K. Eshraghian, "Characterization of crosstalk between CMOS photodiodes", *Solid-State Electronics*. Vol. 46, pp 53-59, 2002.
- [7] Lincoln Bollschweiler, Alex English, R. Jacob Baker, Wang Kuang, Zi-Chang Chang, Ming Hsiung Shih, William B. Knowlton, William L. Hughes, Jeunghoon Lee, Bernard Yurke, Nankyoung Suh Cockerham and Vence C (2009), Tyree. "Chip-Scale Nanophotonic, Chemical and Biological Sensors using CMOS process", Circuits and Systems, 2009. MWSCAS '09. 52nd IEEE International Midwest Symposium, pp 913 – 916, 2009.
- [8] Wenjie Liang, Marc Bockrath, Dolores Bozovic, Jason H. Hafner, M. Tinkham and Hongkun Park (2001), "Fabry-Perot interference in a nanotube electron waveguide", *Journal of Nature*, Vol. 411, No. 7, pp. 665-669.